THREE-LOOP HEAVY QUARK VACUUM POLARIZATION*

K.G. Chetyrkin[a], J.H. Kühn[b], M. Steinhauser[b]

[a] *Max-Planck-Institut für Physik, Werner-Heisenberg-Institut, D-80805 Munich, Germany*
and
Institute for Nuclear Research, Russian Academy of Sciences, Moscow 117312, Russia

[b] *Institut für Theoretische Teilchenphysik, Universität Karlsruhe, D-76128 Karlsruhe, Germany*

Abstract

The real and imaginary part of the vacuum polarization function $\Pi(q^2)$ induced by a massive quark is calculated in perturbative QCD up to order α_s^2. We combine the information from small and large momentum region and from the threshold using conformal mapping and Padé approximation. This leads us to formulae for $\Pi(q^2)$ valid for arbitrary m^2/q^2. Taking subsequently the imaginary part we get the $\mathcal{O}(\alpha_s^2)$ to $R \equiv \sigma(e^+e^- \to \text{hadrons})/\sigma(e^+e^- \to \mu^+\mu^-)$. This extends the calculation by Källén and Sabry from two to three loops.

*Presented by M. Steinhauser.

1 Introduction

The measurement of the total cross section for electron positron annihilation into hadrons allows for a unique test of pertubative QCD. The decay rate $\Gamma(Z \to \text{hadrons})$ provides one of the most precise determinations of the strong coupling constant α_s. In the high energy limit the quark masses can often be neglected. In this approximation QCD corrections to $R \equiv \sigma(e^+e^- \to \text{hadrons})/\sigma(e^+e^- \to \mu^+\mu^-)$ have been calculated up to order α_s^3 [1, 2]. For precision measurements the dominant mass corrections must be included through an expansion in m^2/s. Terms up to order $\alpha_s^3 m^2/s$ [3] and $\alpha_s^2 m^4/s^2$ [4] are available at present, providing an acceptable approximation from the high energy region down to intermediate energy values. For a number of measurements, however, the information on the complete mass dependence is desirable. This includes charm and bottom meson production above the resonance region, say above 4.5 GeV and 12 GeV, respectively, and, of course, top quark production at a future electron positron collider.

To order α_s this calculation was performed by Källén and Sabry in the context of QED a long time ago [5]. With measurements of ever increasing precision, predictions in order α_s^2 are needed for a reliable comparison between theory and experiment. Furthermore, when one tries to apply the $\mathcal{O}(\alpha)$ result to QCD, with its running coupling constant, the choice of scale becomes important. In fact, the distinction between the two intrinsically different scales, the relative momentum versus the center of mass energy, is crucial for a stable numerical prediction. This information can be obtained from a full calculation to order α_s^2 only. Such a calculation then allows to predict the cross section in the complete energy region where perturbative QCD can be applied — from close to threshold up to high energies.

In this contribution results for the cross section are presented in order α_s^2. They are obtained from the vacuum polarization $\Pi(q^2)$ which is calculated up to three loops. The imaginary part of the "fermionic contribution" — derived from diagrams with a massless quark loop inserted in the gluon propagator — has been calculated in [6]. All integrals could be performed to the end and the result was expressed in terms of polylogarithms. In this paper the calculation is extended to the full set of diagrams relevant for QCD. Instead of trying to perform the integrals analytically, we use information of $\Pi(q^2)$ from the large q^2 behaviour, the expansion around $q^2 = 0$ and from threshold. Only results without renormalization group improvement and resummation of the Coulomb singularities from higher orders are presented. Resummation of leading higher order terms, phenomenological applications and a more detailed discussion of our methods will be presented elsewhere.

2 Outline of the Calculation

The different behaviour at threshold makes it necessary to decompose Π according to its colour structure. It is convenient to write:

$$\Pi(q^2) = \Pi^{(0)}(q^2) + \frac{\alpha_s(\mu^2)}{\pi} C_F \Pi^{(1)}(q^2) + \left(\frac{\alpha_s(\mu^2)}{\pi}\right)^2 \Pi^{(2)}(q^2) + \cdots, \tag{1}$$

$$\Pi^{(2)} = C_F^2 \Pi_A^{(2)} + C_A C_F \Pi_{NA}^{(2)} + C_F T n_l \Pi_l^{(2)} + C_F T \Pi_F^{(2)}. \tag{2}$$

The same notation is adopted to the physical observable $R(s)$ which is related to $\Pi(q^2)$ by

$$R(s) = 12\pi \, \mathrm{Im}\Pi(q^2 = s + i\epsilon). \tag{3}$$

The contributions from diagrams with n_l light or one massive internal fermion loop are denoted by $C_F T n_l \Pi_l^{(2)}$ and $C_F T \Pi_F^{(2)}$, respectively. The purely gluonic corrections are proportional to C_F^2 or $C_A C_F$ where the former are the only contributions in an abelian theory and the latter are characteristic for the nonabelian aspects of QCD.

All steps described below have been performed seperately for the first three contributions to $\Pi^{(2)}$. In fact, new information is only obtained for $\Pi_A^{(2)}$ and $\Pi_{NA}^{(2)}$ since $\mathrm{Im}\Pi_l^{(2)}$ is already known analytically [6]. The contribution from a four particle cut with threshold at $4m$ is given in terms of a two dimensional integral [6] which can be solved easily numerically, so $\Pi_F^{(2)}$ will not be treated in this paper. Also the contributions to $\Pi(q^2)$ and $R(s)$ which originate from diagrams where the electromagnetic current couples to a massless quark and the massive quark is produced through a virtual gluon will not be discussed here. They have been calculated in [7]. In the following the behaviour of $\Pi(q^2)$ in the three different kinematical regions and the approximation method is discussed.

Analysis of the high q^2 behaviour

The high energy behaviour of Π provides important constraints on the complete answer. In the limit of small m^2/q^2 the constant term and the one proportional to m^2/q^2 (modulated by powers of $\ln\mu^2/q^2$) have been calculated a long time ago [8]. For the imaginary part even the m^4/q^4 terms are available [4]. This provides an important test of the numerical results presented below.

Threshold behaviour

General arguments based on the influence of Coulomb exchange close to threshold, combined with the information on the perturbative QCD potential and the running of α_s dictate the singularities and the structure of the leading cuts close to threshold, that is for small $v = \sqrt{1-4m^2/s}$. The C_F^2 term is directly related to the QED result with internal photon lines only. The leading $1/v$ singularity and the constant term of R_A can be predicted from the nonrelativistic Greens function for the Coulomb potential and the $\mathcal{O}(\alpha_s)$ calculation. The next-to-leading term is determined by the combination of one loop results again with the Coulomb singularities [10, 11, 12]. One finds

$$R_A^{(2)} = 3\left(\frac{\pi^4}{8v} - 3\pi^2 + \ldots\right). \tag{4}$$

The contributions $\sim C_A C_F$ and $\sim C_F T n_l$ can be treated in parallel. For these colour structures the perturbative QCD potential [9]

$$V_{\mathrm{QCD}}(\vec{q}^{\,2}) = -4\pi C_F \frac{\alpha_V(\vec{q}^{\,2})}{\vec{q}^{\,2}}, \tag{5}$$

$$\alpha_V(\vec{q}^{\,2}) = \alpha_s(\mu^2)\left[1 + \frac{\alpha_s(\mu^2)}{4\pi}\left(\left(\frac{11}{3}C_A - \frac{4}{3}Tn_l\right)\left(-\ln\frac{\vec{q}^{\,2}}{\mu^2} + \frac{5}{3}\right) - \frac{8}{3}C_A\right)\right] \tag{6}$$

will become important. The leading $C_A C_F$ and $C_F T n_l$ term in R is proportional to $\ln v$ and is responsible for the evolution of the coupling constant close to threshold. Also the constant term can be predicted by the observation, that the leading term in order α_s is induced by the potential. The $\mathcal{O}(\alpha_s)$ result

$$R = 3\frac{v(3-v^2)}{2}\left(1 + C_F\frac{\pi^2(1+v^2)}{2v}\frac{\alpha_s}{\pi} + \ldots\right) \tag{7}$$

is employed to predict the logarithmic and constant $C_F C_A$ and $C_F T n_l$ terms of $\mathcal{O}(\alpha_s^2)$ by replacing α_s by $\alpha_V(4\vec{p}^{\,2} = v^2 s)$ as given in Eq.(6). This implies the following threshold behaviour:

$$R_{NA}^{(2)} = 3\frac{\pi^2}{3}(3-v^2)(1+v^2)\left(-\frac{11}{16}\ln\frac{v^2 s}{\mu^2} + \frac{31}{48} + \ldots\right), \tag{8}$$

$$R_l^{(2)} = 3\frac{\pi^2}{3}(3-v^2)(1+v^2)\left(\frac{1}{4}\ln\frac{v^2 s}{\mu^2} - \frac{5}{12} + \ldots\right). \tag{9}$$

This ansatz can be verified for the $C_F T n_l$ term since in this case the result is known in analytical form [6]. Extending the ansatz from the behaviour of the imaginary part close to the branching point into the complex plane allows to predict the leading term of $\Pi(q^2) \sim \ln v$ and $\sim \ln^2 v$.

Behaviour at $q^2 = 0$

Important information is contained in the Taylor series of $\Pi(q^2)$ around zero. The calculation of the first seven nontrivial terms is based on the evaluation of three-loop tadpole integrals with the help of the algebraic program MATAD written in FORM [13] which performs the traces, calculates the derivatives with respect to the external momenta. It reduces the large number of different integrals to one master integral and a few simple ones through an elaborate set of recursion relations based on the integration-by-parts method [14, 15]. The result can be written in the form:

$$\Pi^{(2)} = \frac{3}{16\pi^2} \sum_{n>0} C_n^{(2)} \left(\frac{q^2}{4m^2}\right)^n, \tag{10}$$

where the first seven moments are listed in [16].

Conformal mapping and Padé approximation

The vacuum polarization function $\Pi^{(2)}$ is analytic in the complex plane cut from $q^2 = 4m^2$ to $+\infty$. The Taylor series in q^2 is thus convergent in the domain $|q^2| < 4m^2$ only. The conformal mapping which corresponds to the variable transformation

$$\omega = \frac{1 - \sqrt{1 - q^2/4m^2}}{1 + \sqrt{1 - q^2/4m^2}}, \qquad \frac{q^2}{4m^2} = \frac{4\omega}{(1+\omega)^2}, \tag{11}$$

transforms the cut complex q^2 plane into the interior of the unit circle. The special points $q^2 = 0, 4m^2, -\infty$ correspond to $\omega = 0, 1, -1$, respectively.

The upper (lower) part of the cut is mapped onto the upper (lower) perimeter of the circle. The Taylor series in ω thus converges in the interior of the unit circle. To obtain predictions for $\Pi(q^2)$ at the boundary it has been suggested [17, 18] to use the Padé approximation which converges towards $\Pi(q^2)$ even on the perimeter. To improve the accuracy the singular threshold behaviour and the large q^2 behaviour is incorporated into simple analytical functions which are removed from $\Pi^{(2)}$ before the Padé approximation is performed. The quality of this procedure can be tested by comparing the prediction with the known result for $\mathrm{Im}\Pi_l^{(2)}$.

The logarithmic singularities at threshold and large q^2 are removed by subtraction, the $1/v$ singularity, which is present for the C_F^2 terms only, by multiplication with v as suggested in [12]. The imaginary part of the remainder which is actually approximated by the Padé method is thus smooth in the entire circle, numerically small and vanishes at $\omega = 1$ and $\omega = -1$.

3 Results

After performing the Padé approximation for the smooth remainder with ω as natural variable, the transformation (11) is inverted and the full vacuum polarization function reconstructed by reintroducing the threshold and high energy terms. This procedure provides real and imaginary parts of $\Pi^{(2)}$. Subsequently only the absorbtive part of $\Pi^{(2)}$ (multiplied by 12π) will be presented.

In Fig. 1(a) the complete results are shown for $\mu^2 = m^2$ with $R_A^{(2)}$, $R_{NA}^{(2)}$ and $R_l^{(2)}$ displayed separately. The solid line represents the full correction. The threshold approximation is given by the dotted curve. In the high energy region besides the corrections containing the m^2/s terms (dash-dotted line) also the quartic (dashed line) approximations are shown. It should be stressed that they are not

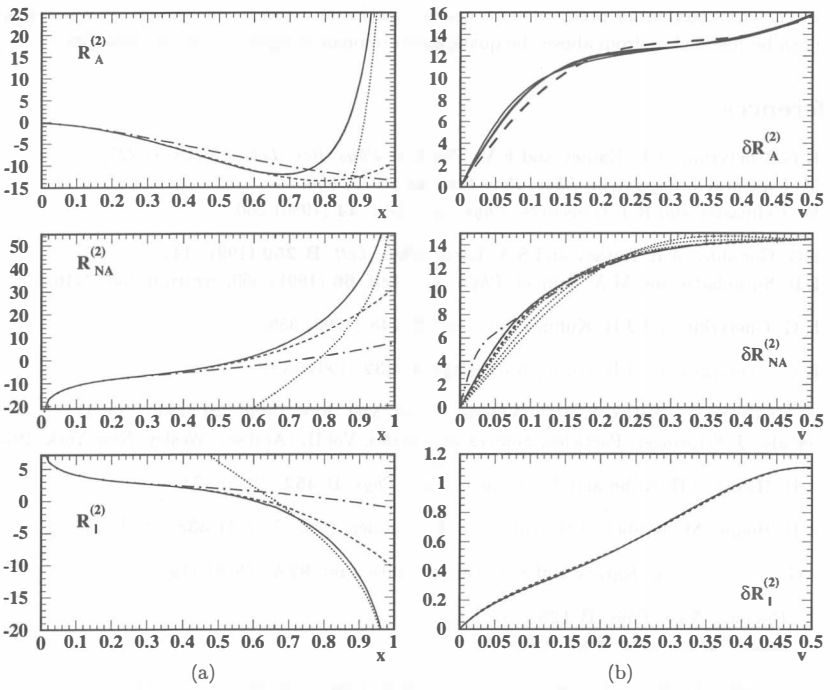

Figure 1: In (a) the complete results (full line) are compared to the threshold approximations and the high energy approximations including the m^2/s (dash-dotted) and the m^4/s^2 (dashed) terms ($x = 2m/\sqrt{s}$). In (b) the threshold behaviour of the remainder δR for three different Padé approximants is shown. (The singular and constant parts around threshold are subtracted.)

incorporated into the construction of $R^{(2)}$ but they are evidently very well reproduced by the method presented here.

Different Padé approximations of the same degree and approximants with a reduced number of parameters give rise to practically indentical predictions, which could hardly be distinguished in Fig. 1(a). Minor variations are observed close to threshold, *after* subtracting the singular and constant parts. The remainder δR for up to ten different Padé approximants is shown in Fig. 1(b). There is a perfect agreement for $R_l^{(2)}$. It is hard to detect the exact result which is represented by the dotted line. $R_{NA}^{(2)}$ seems to converge to the solid line ([4/4], [5/3] and [3/5]) when more moments from small q^2 are included. The dashed lines are from the [3/3], [4/2], [2/4] and [3/4], the dotted ones from lower order Padé approximants. The dash-dotted curve is the [4/3] Padé approximant and has a pole very close to $\omega = 1(1.07\ldots)$. For the abelian part a classification of the different results can be seen: the dashed lines are [4/2] and [2/4], the solid ones [3/2], [2/3], [5/3], [3/5] and [5/4] Padé approximants.

To summarize: Real and imaginary part of the vacuum polarization function $\Pi(q^2)$ from a massive quark have been calculated up to three loops for QCD and QED. This result extends the classic calculations of Källén and Sabri [5] to next-to-leading order. The imaginary part can be used to

predict the cross section for production of massive quarks for arbitrary m^2/s, wherever perturbative QCD can be justified — from above the quarkonium resonance region up to high energies.

References

[1] K.G. Chetyrkin, A.L. Kataev and F.V. Tkachov, *Phys. Rev. Lett.* **85** (1979) 227;
M. Dine and J. Sapirstein, *Phys. Rev. Lett.* **43** (1979) 668;
W. Celmaster and R.J. Gonsalves, *Phys. Rev. Lett.* **44** (1980) 560.

[2] S.G. Gorishny, A.L. Kataev and S.A. Larin, *Phys. Lett.* **B 259** (1991) 144;
L.R. Surguladze and M.A. Samuel, *Phys. Rev. Lett.* **66** (1991) 560; erratum ibid, 2416.

[3] K.G. Chetyrkin and J.H. Kühn, *Phys. Lett.* **B 248** (1990) 359.

[4] K.G. Chetyrkin and J.H. Kühn, *Nucl. Phys.* **B 432** (1994) 337.

[5] G. Källén and A. Sabry, K. Dan. Vidensk. Selsk. Mat.-Fys. Medd. **29** (1955) No. 17,
see also J. Schwinger, Particles, *Sources and Fields*, Vol.II, (Addison-Wesley, New York, 1973).

[6] A.H. Hoang, J.H. Kühn and T. Teubner, *Nucl. Phys.* **B 452** (1995) 173.

[7] A.H. Hoang, M. Jeżabek, J.H. Kühn and T. Teubner, *Phys. Lett.* **B 338** (1994) 330.

[8] S.G. Gorishny, A.L. Kataev and S.A. Larin, *Nouvo Cim.* **92A** (1986) 119.

[9] W. Fischler, *Nucl. Phys.* **B 129** (1977) 157;
A. Billoire, *Phys. Lett.* **B 92** (1980) 343.

[10] R. Barbieri, R. Gatto, R. Kögerler and Z. Kunszt, *Phys. Lett.* **B 57** (1975) 455.

[11] B. H. Smith and M.B. Voloshin, *Phys. Lett.* **B 324** (1994) 117; erratum ibid, **B 333** (1994) 564.

[12] P.A. Baikov and D.J. Broadhurst, Report Nos. OUT-4102-54, INP-95-13/377 and
hep-ph/9504398, to appear in *New Computing Techniques in Physics Research IV*, (World Scientific, in press).

[13] J.A.M. Vermaseren, *Symbolic Manipulation with FORM*, (Computer Algebra Netherlands, Amsterdam, 1991).

[14] F.V. Tkachov, *Phys. Lett.* **B 100** (1981) 65;
K.G. Chetyrkin and F.V. Tkachov, *Nucl. Phys.* **B 192** (1981) 159.

[15] D.J. Broadhurst, *Z. Phys.* **C 54** (1992) 54.

[16] K.G. Chetyrkin, J.H. Kühn and M. Steinhauser, *Phys. Lett.* **B 371** (1996) 93;
K.G. Chetyrkin, J.H. Kühn and M. Steinhauser, in preparation.

[17] J. Fleischer and O.V. Tarasov, *Z. Phys.* **C 64** (1994) 413.

[18] D.J. Broadhurst, J. Fleischer and O.V. Tarasov, *Z. Phys.* **C 60** (1993) 287.